



ELSEVIER

Nuclear Physics B 643 (2002) 367–390

NUCLEAR
PHYSICS B

www.elsevier.com/locate/npe

Cosmic microwave background, matter–antimatter asymmetry and neutrino masses

W. Buchmüller^a, P. Di Bari^a, M. Plümacher^b

^a *Deutsches Elektronen-Synchrotron DESY, 22603 Hamburg, Germany*

^b *Theoretical Physics, University of Oxford, 1 Keble Road, Oxford, OX1 3NP, United Kingdom*

Received 12 June 2002; received in revised form 29 July 2002; accepted 12 August 2002

Abstract

We study the implications of thermal leptogenesis for neutrino parameters. Assuming that decays of N_1 , the lightest of the heavy Majorana neutrinos, initiate baryogenesis, we show that the final baryon asymmetry is determined by only four parameters: the CP asymmetry ε_1 , the heavy neutrino mass M_1 , the effective light neutrino mass \tilde{m}_1 , and the quadratic mean \bar{m} of the light neutrino masses. Imposing the CMB measurement of the baryon asymmetry as constraint on the neutrino parameters, we show, in a model independent way, that quasi-degenerate neutrinos are incompatible with thermal leptogenesis. For maximal CP asymmetry ε_1 , and neutrino masses in the range from $(\Delta m_{\text{sol}}^2)^{1/2}$ to $(\Delta m_{\text{atm}}^2)^{1/2}$, the baryogenesis temperature is $T_B = \mathcal{O}(10^{10})$ GeV.

© 2002 Elsevier Science B.V. All rights reserved.

PACS: 98.80.Cq; 13.35.Hb; 14.60.Pq; 14.60.St

1. Introduction

The explanation of the cosmological baryon asymmetry is a challenge for particle physics. In principle, already the standard model contains all necessary ingredients, baryon number violation, C and CP violation, and also the required departure from thermal equilibrium could be generated during the electroweak phase transition [1]. However, due to the lower bound on the Higgs boson mass from LEP, electroweak baryogenesis is no longer a viable mechanism, except for some supersymmetric extensions of the standard model [2].

E-mail address: pluemi@thphys.ox.ac.uk (M. Plümacher).

A simple and elegant explanation of the observed baryon asymmetry is offered by neutrino physics. During the past years data on atmospheric and solar neutrinos have provided strong evidence for neutrino masses and mixings. In the seesaw mechanism [3] the smallness of these neutrino masses is naturally explained by the mixing of the left-handed neutrinos with heavy Majorana neutrinos. Further, the connection between baryon and lepton number in the high-temperature, symmetric phase of the standard model due to rapid sphaleron transitions [4] is by now firmly established [5]. As in classical GUT baryogenesis [6], out-of-equilibrium decays of the heavy Majorana neutrinos can then generate a lepton asymmetry which, by sphaleron processes, is partially transformed into a baryon asymmetry [7].

A beautiful aspect of this ‘leptogenesis’ mechanism is the connection between the cosmological baryon asymmetry and neutrino properties. This connection is established by standard kinetic calculations [8,9], very much like in big-bang nucleosynthesis [6], where light nuclei play the role analogous to leptons in leptogenesis. The requirement of ‘successful baryogenesis’, i.e., the existence of neutrino masses and mixings for which the predicted and the observed value of the baryon asymmetry are in agreement, constitutes a severe test for models of neutrino masses, which has been extensively explored during the past years [10].

On the experimental side, the precision of measurements of the baryon asymmetry has significantly improved with the observation of the acoustic peaks in the cosmic microwave background radiation (CMB). The BOOMERanG and DASI experiments have measured the baryon asymmetry with a (1σ) standard error of $\sim 15\%$ [11,12],

$$(\Omega_B h^2)^{\text{CMB}} = 0.022^{+0.004}_{-0.003}. \quad (1)$$

Since the number of relic photons per comoving volume is very unlikely to have changed after recombination, this is easily translated into a measurement of the quantity $\eta_B = (n_B/n_\gamma)$ at the present time,

$$\eta_{B0}^{\text{CMB}} = (6.0^{+1.1}_{-0.8}) \times 10^{-10}. \quad (2)$$

The MAXIMA experiment finds a 95% c.l. range $(\Omega_b h^2)^{\text{CMB}} = 0.033 \pm 0.013$ [13], corresponding to $\eta_{B0}^{\text{CMB}} = (9.0 \pm 3.6) \times 10^{-10}$. The CBI experiment finds a 1σ range $(\Omega_b h^2)^{\text{CMB}} = 0.022^{+0.015}_{-0.009}$ [14], corresponding to $\eta_{B0}^{\text{CMB}} = (6.0^{+4.1}_{-2.5}) \times 10^{-10}$. When a combined analysis of all four experiments is performed [14], the result almost coincides with the one in Eq. (2). The four experiments use different techniques, and it is remarkable that their results are consistent with each other. In the near future the MAP experiment will provide results of the first full sub-degree sky survey of temperature anisotropies [15]. The expected (1σ) standard error on η_{B0} is $\sim 10\%$, using only CMB data, no polarization measurement and even allowing for the presence of gravity wave perturbations [16]. The Planck satellite, whose launch is planned for 2007 [17], should reduce this error to $\sim 1\%$. If the polarization will be measured, and if it will be possible to add extra CMB information on other cosmological parameters, then the error may become even less than 1% [16].

The CMB measurement of the baryon asymmetry has to be compared with the result of standard BBN, obtained from the measurement of relic nuclear abundances, which gives the range $\eta_{B0}^{\text{SBBN}} = (2.6\text{--}6.2) \times 10^{-10}$ [18]. This is in good agreement with the CMB range,

in particular with the 3σ lower limit obtained from Eq. (2) which will be particularly important to our analysis.

In the following we shall calculate the baryon asymmetry by solving the Boltzmann equations given in [8,9], assuming that the dominant contribution is given by decays of N_1 , the lightest of the heavy Majorana neutrinos. This assumption is well justified in the case of a mass hierarchy among the heavy neutrinos, i.e., $M_1 \ll M_2, M_3$, and it is also known to be a good approximation, if $M_{2,3} - M_1 = \mathcal{O}(M_1)$ [19]. The case $M_{2,3} - M_1 \ll M_1$ requires a special treatment. For some flavour structures of the neutrino mass matrices it is also conceivable that the decays of the heavier neutrinos N_2 or N_3 are the main source of the baryon asymmetry [20]. In our analysis we shall assume that quantum corrections [21] to the Boltzmann equations are small. So far, no detailed quantitative study of this important question has been carried out.

As we shall see, within this framework one is left with only four parameters: M_1 , the CP asymmetry ε_1 , the effective neutrino mass \tilde{m}_1 and \bar{m} , the quadratic mean of the light neutrino masses. For each set of values of these four parameters the Boltzmann equations yield a prediction for the baryon asymmetry. A comparison with the observed value then defines an allowed region in the space of neutrino parameters.

In addition to the neutrino parameters, there are also three quantities which characterize the initial conditions: the initial temperature, the initial abundance of heavy neutrinos and, of course, the initial baryon asymmetry. A detailed study of the stability of the final baryon asymmetry under variations of these initial conditions will be presented elsewhere [19]. In the following we shall illustrate this dependence by presenting all results for two different choices of the initial N_1 abundance, namely, zero and thermal initial abundance. All values in-between can be estimated by interpolation between these two cases. One can also easily extrapolate the results to initial N_1 abundances higher than the thermal one. Fortunately, for the most interesting range of \tilde{m}_1 the dependence on the initial N_1 abundance turns out to be very small. Clearly, a theory of the very early universe, like inflation, is needed to calculate the initial conditions for baryogenesis.

The paper is organized as follows. In Section 2 we recall the Boltzmann equations which we then solve numerically. We also briefly discuss some approximations underlying these equations. Section 3 deals with the theoretically allowed range of the neutrino parameters, in particular, the upper bound on the CP asymmetry. In Section 4 we present our numerical results for the baryon asymmetry and discuss the dependence on the neutrino parameters and on the choice of the initial condition. We then investigate the constraints imposed by the CMB result on the neutrino parameters. Our conclusions are given in Section 5.

2. Solutions of the Boltzmann equations

The dynamical generation of a baryon asymmetry requires that the particle interactions do not conserve baryon number, C and CP. In leptogenesis these conditions are realized by the couplings of the heavy Majorana neutrinos N_i . Their decays can generate an asymmetry in the number of leptons and antileptons, and therefore in $B-L$. The crucial departure from thermal equilibrium is provided by the expansion of the universe. At temperatures

$T \sim \mathcal{O}(M_1)$ the abundance of heavy neutrinos exceeds the thermal abundance due to their weak interactions with the thermal bath.

A quantitative description of this non-equilibrium process is obtained by means of kinetic equations. The relevant processes in the thermal plasma are:

- N_1 decays (D) and inverse-decays (ID) into leptons and Higgs bosons, $N_1 \leftrightarrow \phi l$, and into antileptons and anti-Higgs bosons, $N_1 \leftrightarrow \phi \bar{l}$;
- $\Delta L = 2$ scatterings mediated by the exchange of all heavy Majorana neutrinos, $l\phi \leftrightarrow \bar{l}\bar{\phi}$ (N), and $ll \leftrightarrow \bar{\phi}\bar{\phi}$, $\bar{l}\bar{l} \leftrightarrow \phi\phi$ (N, t);
- $\Delta L = 1$ scatterings, $N_1 l(\bar{l}) \leftrightarrow \bar{l}(t)q(\bar{q})$ (ϕ, s) and $N_1 t(\bar{t}) \leftrightarrow \bar{l}(l)q(\bar{q})$ (ϕ, t);

in brackets we have indicated how the rates of these processes are labeled in the following. In principle, one could also have additional processes, in particular, those which contribute to bring the heavy neutrinos initially into thermal equilibrium [9]. In the present, minimal framework we neglect such interactions.

Since we are assuming that N_1 decays are the origin of lepton and baryon asymmetries, the natural temperature scale is given by the mass M_1 . It is therefore convenient to measure temperature in units of M_1 and to introduce the dimensionless variable $z = M_1/T$. For realistic values $M_1 \gg 100$ GeV, all standard model particles can be treated as massless, and we shall assume that they are in thermal equilibrium.

The time evolution of a charge density or a number density n_X depends on the microphysical processes in the thermal plasma as well as the expansion of the universe. For the discussion of leptogenesis it is convenient to consider instead of the number density n_X the particle number N_X in some portion of comoving volume, which takes the effect of the expansion automatically into account. We choose the comoving volume $R_\star(t)^3$ which contains one photon at time t_\star before the onset of leptogenesis,

$$N_X(t) = n_X(t) R_\star(t)^3, \quad (3)$$

with

$$R_\star(t_\star) = (n_\gamma^{\text{eq}}(t_\star))^{-1/3}, \quad (4)$$

and therefore $N_\gamma(t_\star) = 1$. For a boson with g_B degrees of freedom one has $N_B(t_\star) = g_B/2$, whereas for a fermion with g_F degrees of freedom $N_F(t_\star) = 3g_F/8$. Alternatively, one may normalize the number density to the entropy density s and consider $Y_X = n_X/s$, as frequently done in the literature. If entropy is conserved, both normalizations are related by a constant. However, an inconvenient aspect of the quantity Y_X is its dependence on the entropy degrees of freedom, $g_S(t_\star)/g_S(t_0)$, and on possible entropy production between t_\star and t_0 .

The final baryon asymmetry is conveniently expressed in terms of the baryon-to-photon ratio $\eta_{B0} = n_B(t_0)/n_\gamma(t_0)$, to be compared with the CMB measurement (2). The predicted value of η_{B0} is obtained from N_B^0 by accounting for the dilution factor $f = N_\gamma(t_0) > 1$,

$$\eta_{B0} = \frac{1}{f} N_B^0. \quad (5)$$

In the simple case of constant entropy one has $f = g_S^*/g_S^0$, with $g_S^0 = 2 + 21/11 \simeq 3.91$. Assuming at t_* the standard model degrees of freedom with a single Majorana neutrino in addition, one obtains $g_S^* = 434/4$, and therefore $\eta_{B0} \simeq 0.036 N_{B0}$.

In the decays of the heavy Majorana neutrinos an asymmetry in the number of lepton doublets, and therefore in $B-L$, is generated. In the following we shall sum over the three lepton numbers L_e, L_μ and L_τ . Because of the large neutrino mixings suggested by the solar and atmospheric neutrino anomalies, we expect this to be a good approximation. A refined analysis can be performed along the lines discussed in Ref. [22]. A related problem is the role of ‘spectator processes’ [23] which change the naive sphaleron baryon-to-lepton conversion rate by a factor $\mathcal{O}(1)$, since any generated asymmetry in lepton doublets is fast distributed among many leptonic and baryonic degrees of freedom in the plasma. In the following we shall ignore this uncertainty and use the naive sphaleron conversion factor for N_B/N_{B-L} , which in the standard model with one Higgs doublet is $a = 28/79 \simeq 0.35$ [24]. The baryon-to-photon ratio today is then given by

$$\eta_{B0} \simeq 0.013 N_{B-L}^0. \quad (6)$$

The Boltzmann equations for the time evolution of the number of heavy Majorana neutrinos, N_1 , and of $B-L$ number, N_{B-L} , are given by [8,9],

$$\frac{dN_{N_1}}{dt} = -(\Gamma_D + \Gamma_S)(N_{N_1} - N_{N_1}^{\text{eq}}), \quad (7)$$

$$\frac{dN_{B-L}}{dt} = -\varepsilon_1 \Gamma_D (N_{N_1} - N_{N_1}^{\text{eq}}) - \Gamma_W N_{B-L}. \quad (8)$$

Here the rate Γ_D accounts for decays and inverse decays ($z = M_1/T$),

$$\Gamma_D = \frac{1}{8\pi} (h^\dagger h)_{11} M_1 \frac{K_1(z)}{K_2(z)}, \quad (9)$$

where K_1 and K_2 are Bessel functions, and h is the Dirac neutrino Yukawa matrix (cf. Section 3); the inverse decay rate is given by $\Gamma_{\text{ID}} = (n_{N_1}^{\text{eq}}/n_l) \Gamma_D$.

The N_1 scattering rate involves processes with the Higgs field ϕ in t - and s -channel,

$$\Gamma_S = 2\Gamma_{\phi,t}^{(N_1)} + 4\Gamma_{\phi,s}^{(N_1)}. \quad (10)$$

Inverse decays, $\Delta L = 1$ processes ($\Gamma_{\phi,t}, \Gamma_{\phi,s}$) and $\Delta L = 2$ processes ($\Gamma_N, \Gamma_{N,t}$) all contribute to the washout rate,

$$\Gamma_W = \left(\frac{1}{2} \Gamma_{\text{ID}} + 2\Gamma_{\phi,t}^{(l)} + \Gamma_{\phi,s}^{(l)} \frac{N_{N_1}}{N_{N_1}^{\text{eq}}} \right) + 2\Gamma_N^{(l)} + 2\Gamma_{N,t}^{(l)}. \quad (11)$$

The quantities $\Gamma_i^{(X)}$ are thermally averaged reaction rates per particle X . They are related by $\Gamma_i^{(X)} = \gamma_i/n_X^{\text{eq}}$ to the reaction densities γ_i [8] which are obtained from the reduced cross sections $\hat{\sigma}_i(s/M_1^2)$,

$$\gamma_{(i)}(z) = \frac{M_1^4}{64\pi^4} \frac{1}{z} \int_{(m_a^2+m_b^2)/M_1^2}^{\infty} dx \hat{\sigma}_{(i)}(x) \sqrt{x} K_1(z\sqrt{x}), \quad (12)$$

where m_a and m_b are the masses of the two particles in the initial state. Our calculations are based on the reduced cross sections given in Ref. [25].

An important part of our analysis is an improved treatment of the $\Delta L = 2$ processes which involve the heavy Majorana neutrinos N_i , $i = 1, \dots, 3$, as intermediate states. The reduced cross sections $\hat{\sigma}_N$ and $\hat{\sigma}_{(N,t)}$ read,

$$\hat{\sigma}_{N(N,t)} = \frac{1}{2\pi} \left[\sum_i (h^\dagger h)_{ii}^2 f_{ii}^{N(N,t)}(x) + \sum_{i < j} \text{Re}(h^\dagger h)_{ij}^2 f_{ij}^{N(N,t)}(x) \right], \quad (13)$$

with

$$f_{ii}^N(x) = 1 + \frac{a_j}{D_j(x)} + \frac{x a_j}{2D_j^2(x)} - \frac{a_j}{x} \left[1 + \frac{x + a_j}{D_j} \right] \ln \left(1 + \frac{x}{a_j} \right), \quad (14)$$

$$\begin{aligned} f_{ij}^N(x) = \sqrt{a_i a_j} & \left[\frac{1}{D_i(x)} + \frac{1}{D_j(x)} + \frac{x}{D_i(x) D_j(x)} \right. \\ & + \left(1 + \frac{a_i}{x} \right) \left(\frac{2}{a_j - a_i} - \frac{1}{D_j(x)} \right) \ln \left(1 + \frac{x}{a_i} \right) \\ & \left. + \left(1 + \frac{a_j}{x} \right) \left(\frac{2}{a_i - a_j} - \frac{1}{D_i(x)} \right) \ln \left(1 + \frac{x}{a_j} \right) \right], \end{aligned} \quad (15)$$

$$f_{ii}^{N,t}(x) = \frac{x}{x + a_j} + \frac{a_j}{x + 2a_j} \ln \left(1 + \frac{x}{a_j} \right), \quad (16)$$

$$\begin{aligned} f_{ij}^{N,t}(x) = \frac{\sqrt{a_i a_j}}{(a_i - a_j)(x + a_i + a_j)} \\ \times \left[(2x + 3a_i + a_j) \ln \left(1 + \frac{x}{a_j} \right) - (2x + 3a_j + a_i) \ln \left(1 + \frac{x}{a_i} \right) \right]. \end{aligned} \quad (17)$$

Here $a_j \equiv M_j^2/M_1^2$, and $1/D_i(x) \equiv (x - a_i)/[(x - a_i)^2 + a_i c_i]$ is the off-shell part of the N_i propagator with $c_i = a_i (h^\dagger h)_{ii}^2 / (8\pi)^2$.

The sum $\gamma_N + \gamma_{N,t}$ is conveniently separated in two parts. The first part comes from the resonance contribution $\propto x/D_1^2$, which is highly peaked around $x = 1$. This term is easily evaluated analytically in the zero-width limit,

$$\gamma_N^{\text{res}} = \frac{M_1^4}{64\pi^3} (h^\dagger h)_{11} \frac{1}{z} K_1(z). \quad (18)$$

For typical values of $(h^\dagger h)_{11}$ and M_1 the resonance contribution dominates in the temperature range from $T \simeq M_1$ ($z \simeq 1$) down to $T \simeq 0.1 M_1$ ($z \simeq 10$). The remaining part is dominant at low temperatures, $z > 10$. For $z \gg 1$ the main contribution to the integrals γ_N and $\gamma_{N,t}$ comes from the region $x \ll 1$. Here the scattering amplitudes with N_i exchange are proportional to the light neutrino mass matrix m_ν . To leading order in x for $\hat{\sigma}_N$ and $\hat{\sigma}_{(N,t)}$, one finds

$$\gamma_N(z \gg 1) \simeq \gamma_{(N,t)}(z \gg 1) \simeq \frac{3M_1^6}{8\pi^5 v^4} \frac{1}{z^6} \text{tr}(m_\nu^\dagger m_\nu). \quad (19)$$

For hierarchical neutrinos $\bar{m}^2 = \text{tr}(m_\nu^\dagger m_\nu) \simeq \Delta m_{\text{atm}}^2$, whereas for quasi-degenerate neutrinos one has $\bar{m}^2 \simeq 3m_1^2$, with $m_1 \simeq m_2 \simeq m_3 \gg \Delta m_{\text{atm}}^2$.

Since all rates are expressed as functions of z , it is convenient to replace time by $z = M_1/T$ in the Eqs. (7) and (8). This change of variables introduces the Hubble parameter since $dt/dz = 1/(Hz)$, with $H \simeq 1.66\sqrt{g_\rho}(M_1^2/M_{\text{Pl}})/z^2$ where g_ρ is the number of energy degrees of freedom at t_* . Neglecting the small variation of the number of degrees of freedom during leptogenesis one obtains for the standard model with one right-handed neutrino $g_\rho = 434/4$.

The kinetic equations for leptogenesis now read,

$$\frac{dN_{N_1}}{dz} = -(D + S)(N_{N_1} - N_{N_1}^{\text{eq}}), \quad (20)$$

$$\frac{dN_{B-L}}{dz} = -\varepsilon_1 D(N_{N_1} - N_{N_1}^{\text{eq}}) - W N_{B-L}, \quad (21)$$

where we have defined $(D, S, W) = (\Gamma_D, \Gamma_S, \Gamma_W)/(Hz)$. In order to understand the dependence of the solutions on the neutrino parameters, it is crucial to note that the rates Γ_D , Γ_S and also Γ_W , except for the contribution $\Delta\Gamma_W = \Gamma_N^{(l)} - \Gamma_{N,\text{res}}^{(l)} + \Gamma_{N,t}^{(l)}$, are all proportional to $(h^\dagger h)_{11}$. The rescaled rates in Eqs. (20) and (21) are therefore dimensionless functions of z , proportional to

$$D, S, W - \Delta W \propto \frac{M_{\text{Pl}}\tilde{m}_1}{v^2}, \quad \Delta W \propto \frac{M_{\text{Pl}}M_1\bar{m}^2}{v^4}; \quad (22)$$

the effective neutrino mass \tilde{m}_1 [9] is given by

$$\tilde{m}_1 = \frac{(m_D^\dagger m_D)_{11}}{M_1}, \quad (23)$$

where m_D is the Dirac neutrino mass matrix (cf. Section 3). Eq. (22) implies that, as long as ΔW can be neglected, the generated lepton asymmetry is independent of M_1 .

Since ΔW increases with M_1 , it does become important at large values of M_1 . At $z \gg 1$, one easily obtains from (19),

$$\Delta W(z \gg 1) = \alpha \frac{M_1\bar{m}^2}{z^2}, \quad (24)$$

with $\alpha^{-1} = \zeta(3)\pi^3 g_I v^4 H(z=1)/M_1^2$.

For $z < 1$, ΔW is no longer proportional to $M_1\bar{m}^2$, but depends on the heavy neutrino masses M_i and on the specific structure of the h matrix. An approximate upper bound Γ_W^+ on Γ_W is given by the sum of the resonance contribution $\Gamma_{N,\text{res}}^{(l)}$ and $\Delta\Gamma(z \gg 1)$ taken at all values of z . In this way the relativistic suppression of N_1 exchange at high temperatures is underestimated. Analogously, a lower limit Γ_W^- can be obtained by treating in the off-shell part $\Delta\Gamma$ the heavy neutrinos N_2 and N_3 kinematically like N_1 , which overestimates the relativistic suppression of $N_{2,3}$ exchange at high temperatures. The two branches Γ_W^\pm are shown in Figs. 1(a)–4(a). As expected, the uncertainty of $\Gamma_W(z)$ at small z is not important for the final baryon asymmetry in most cases. Numerically, we find that is negligible for heavy neutrino masses $M_1 \lesssim 10^{13} \text{ GeV}(0.1 \text{ eV}/\bar{m})^2$.

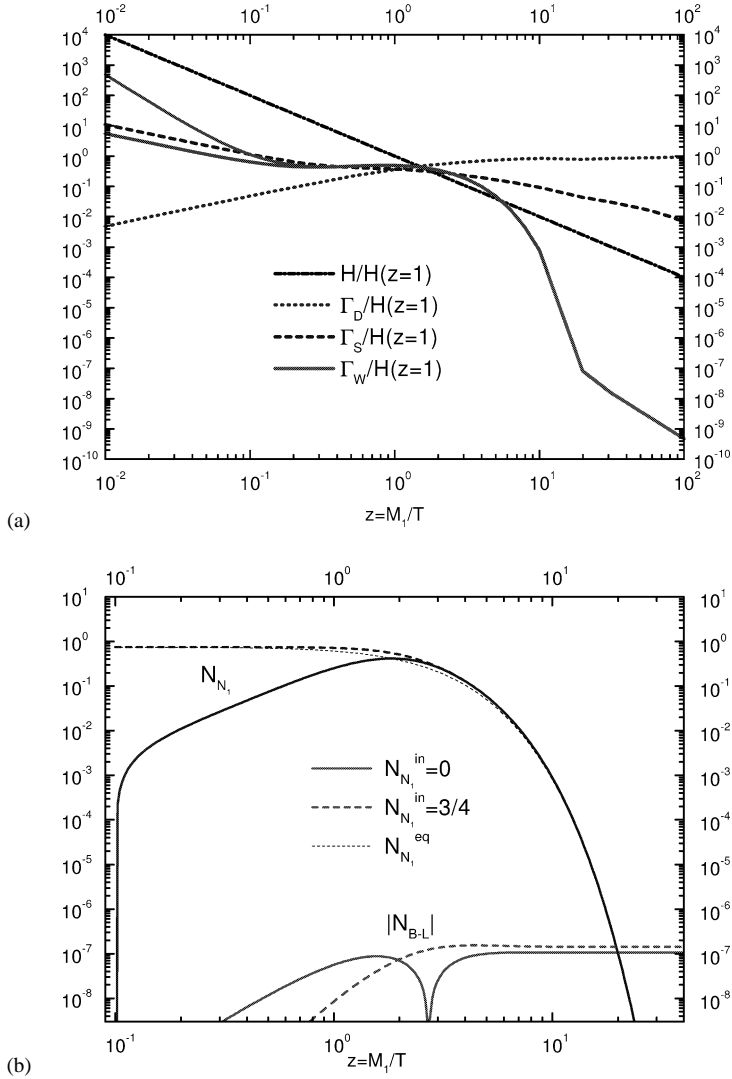


Fig. 1. $M_1 = 10^{10}$ GeV, $\tilde{m}_1 = 10^{-3}$ eV. (a) Rates normalized to the expansion rate at $z = 1$. The two branches for Γ_W at small z correspond to the upper (lower) bounds Γ_W^+ (Γ_W^-) (see text). (b) Evolution of the N_1 abundance and the $B-L$ asymmetry for $\varepsilon_1 = -10^{-6}$ and $\tilde{m} = 0.05$ eV, both zero and thermal initial N_1 abundance.

Successful leptogenesis requires a departure from thermal equilibrium for the decaying heavy Majorana neutrinos. Furthermore, at the same time, washout processes must not be in thermal equilibrium. The corresponding naive out-of-equilibrium conditions are $(\Gamma_D + \Gamma_S)|_{z=1} < H|_{z=1}$ and $\Gamma_W|_{z=1} < H|_{z=1}$. These conditions are fulfilled for a typical set of parameters $M_1 = 10^{10}$ GeV, $\tilde{m}_1 = 10^{-3}$ eV, $\tilde{m} = 0.05$ eV, for which the three rates and the Hubble parameter are shown in Fig. 1(a). The generation of the $B-L$ asymmetry

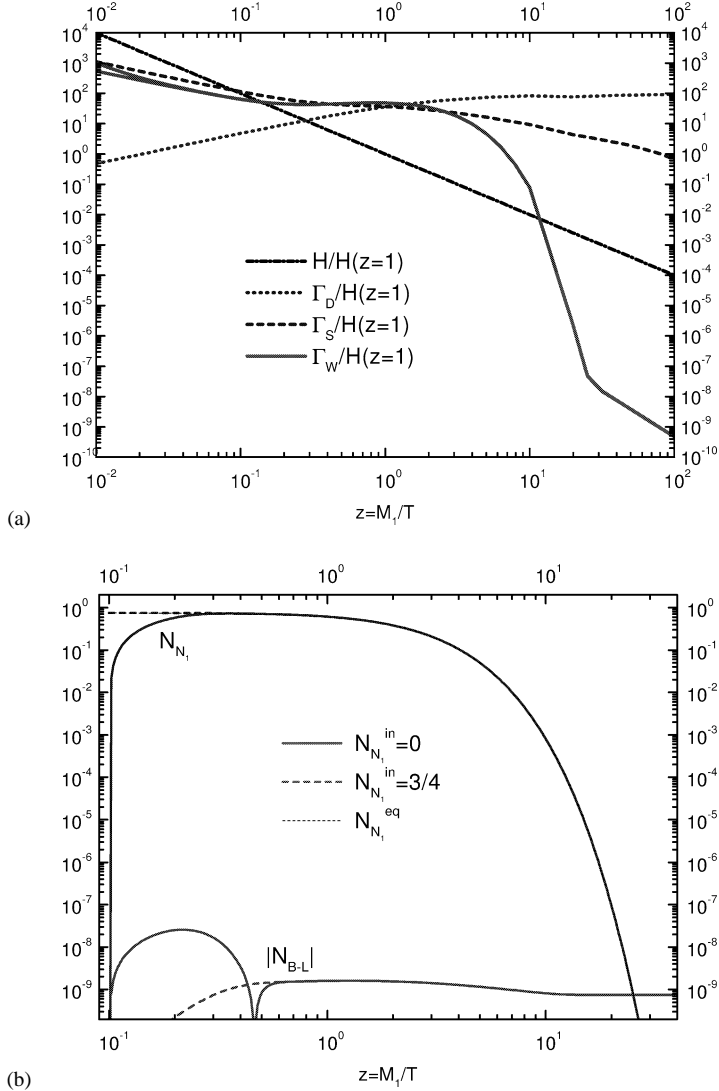


Fig. 2. (a) Rates and (b) evolution of N_1 abundance $B-L$ asymmetry; parameters as in Fig. 1, except $\tilde{m}_1 = 10^{-1}$ eV.

for these parameters is shown in Fig. 1(b) for $|\varepsilon_1| = 10^{-6}$. The figure also demonstrates that the Yukawa interactions are strong enough to bring the heavy neutrinos into thermal equilibrium. The resulting asymmetry is in accord with observation.

Increasing \tilde{m}_1 by two orders of magnitude to $\tilde{m}_1 = 10^{-1}$ eV increases all rates while leaving the Hubble parameter unchanged. As Fig. 2(a) shows, the out-of-equilibrium condition for N_1 decays is now no longer fulfilled, and the final $B-L$ asymmetry is reduced by two orders of magnitude. Increasing M_1 to 10^{15} GeV increases ΔW by five orders of

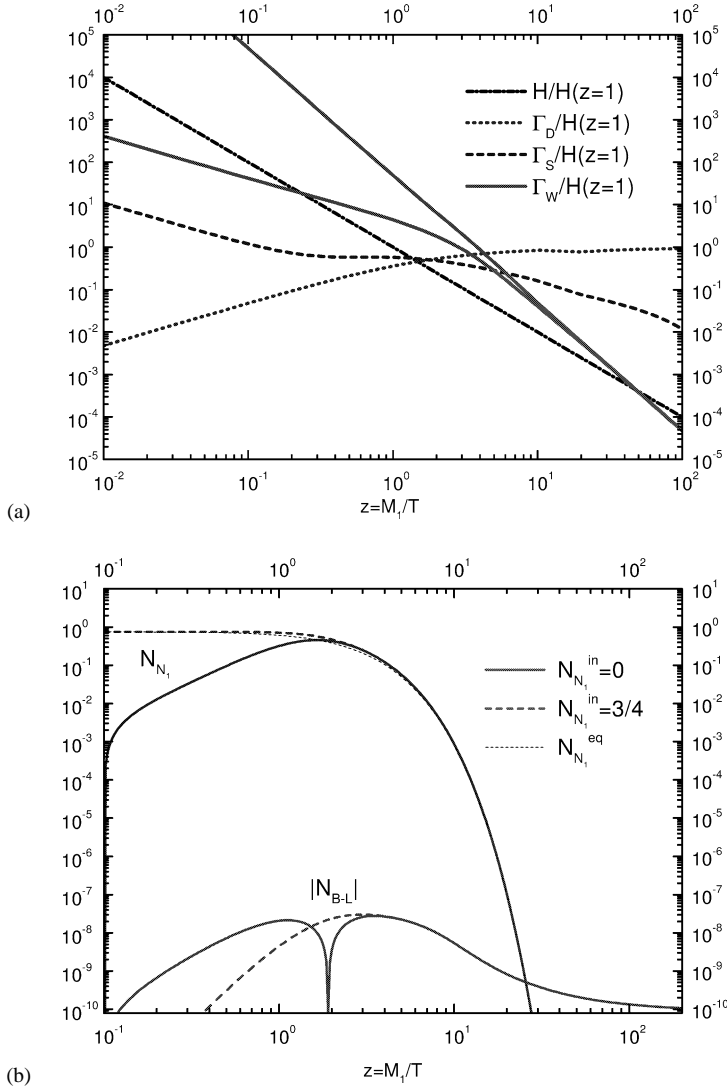


Fig. 3. (a) Rates and (b) evolution of N_1 abundance $B-L$ asymmetry; parameters as in Fig. 1, except $M_1 = 10^{15}$ GeV.

magnitude, which now dominates the shape of the washout rate Γ_W (Fig. 3(a)). Although the Yukawa interactions are strong enough to bring the heavy neutrino into thermal equilibrium, the washout rate is now so large that the final $B-L$ asymmetry is reduced by three orders of magnitude. Even in this extreme case the effect of the uncertainty in ΔW at small z on the final baryon asymmetry is only a factor 2. Finally, reducing \tilde{m}_1 to 10^{-5} eV while keeping $M_1 = 10^{10}$ GeV fixed (Fig. 4(a)), one becomes dependent on the initial conditions. The Yukawa interactions are no longer strong enough to bring the

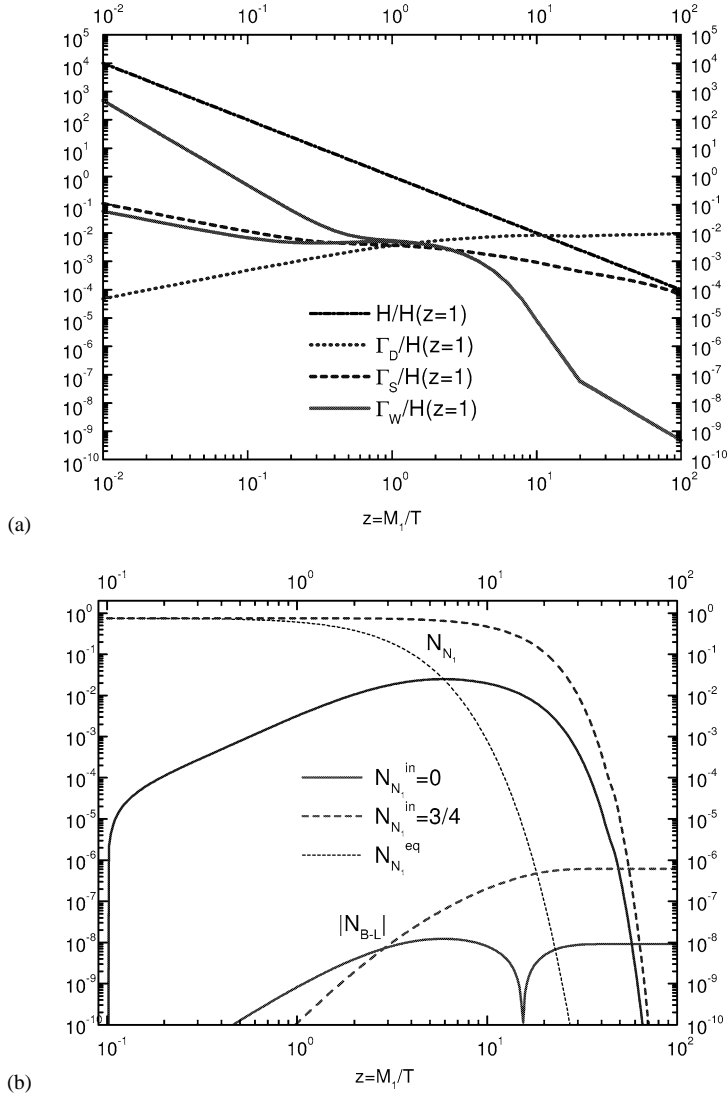


Fig. 4. (a) Rates and (b) evolution of N_1 abundance $B-L$ asymmetry; parameters as in Fig. 1, except $\tilde{m}_1 = 10^{-5}$ eV.

heavy neutrinos into thermal equilibrium (Fig. 4(b)). Starting from zero initial abundance, $N_{N_1}^{in} = 0$, the final $B-L$ asymmetry is reduced by one order of magnitude compared to Fig. 1(b). On the other hand, assuming initially a thermal distribution, which may have been generated by other interactions, the final asymmetry is enhanced by one order of magnitude compared to Fig. 1(b). This is the ‘way-out-of-equilibrium’ case, where washout effects can be neglected, and the final $B-L$ asymmetry is given by $-3\varepsilon_1/4$.

3. The CP asymmetry

Consider now the standard model with right-handed neutrinos. The neutrino masses are obtained from the Lagrangian,

$$\mathcal{L}_m = h_{ij} \bar{l}_{Li} \nu_{Rj} \phi + \frac{1}{2} M_{ij} \bar{\nu}_{Ri}^c \nu_{Rj} + \text{h.c.} \quad (25)$$

Here M is the Majorana mass matrix of the right-handed neutrinos, and the Yukawa couplings h yield the Dirac neutrino mass matrix $m_D = h v$ after spontaneous symmetry breaking, $v = \langle \phi \rangle$. We work in the mass eigenstate basis of the right-handed neutrinos where M is diagonal with real and positive eigenvalues $M_1 \leq M_2 \leq M_3$. The seesaw mechanism [3] then yields for the light neutrino mass matrix,

$$m_\nu = -m_D \frac{1}{M} m_D^T, \quad (26)$$

where higher order terms in $1/M$ have been neglected.

The mass matrix m_ν can again be diagonalized by a unitary matrix $U^{(v)}$,

$$U^{(v)\dagger} m_\nu U^{(v)*} = - \begin{pmatrix} m_1 & 0 & 0 \\ 0 & m_2 & 0 \\ 0 & 0 & m_3 \end{pmatrix} \equiv -D_m, \quad (27)$$

with real and positive eigenvalues satisfying $m_1 \leq m_2 \leq m_3$. Inserting Eq. (26) one finds,

$$v^2 U^{(v)\dagger} h D_M^{-1} h^T U^{(v)*} = D_m, \quad (28)$$

which means that

$$\Omega = v D_m^{-1/2} U^{(v)\dagger} h D_M^{-1/2} \quad (29)$$

is an orthogonal matrix, $\Omega \Omega^T = I$ [26]. This also implies $\text{Im}(\Omega^T \Omega)_{11} = 0$, from which one immediately obtains

$$\frac{1}{m_1} \text{Im}(U^{(v)\dagger} h)_{11}^2 = - \sum_{i \neq 1} \frac{1}{m_i} \text{Im}(U^{(v)\dagger} h)_{i1}^2. \quad (30)$$

The CP asymmetries in the decays of the heavy Majorana neutrinos arise at one-loop order from the interference of the tree level amplitude with vertex and self-energy corrections [27–29]. In the following, we shall restrict ourselves to the case of hierarchical heavy neutrinos, i.e., $M_1 \ll M_2, M_3$. The CP asymmetry ε_1 for the decay of N_1 is then easily obtained by first integrating out the heavier fields N_2 and N_3 . From the tree amplitude and the effective lepton–Higgs interaction one then obtains the useful expression [21],

$$\varepsilon_1 \simeq - \frac{3}{16\pi} \frac{M_1}{(h^\dagger h)_{11}} \text{Im} \left(h^\dagger h \frac{1}{M} h^T h^* \right)_{11}, \quad (31)$$

where corrections $\mathcal{O}(M_1/M_{2,3})$ have been neglected. Using Eqs. (27) and (30) one easily derives,

$$\varepsilon_1 = \frac{3}{16\pi} \frac{M_1}{v^2} \sum_{i \neq 1} \frac{\Delta m_{i1}^2}{m_i} \frac{\text{Im}(\tilde{h}_{i1}^2)}{(\tilde{h}^\dagger \tilde{h})_{11}}, \quad (32)$$

where $\Delta m_{i1}^2 = m_i^2 - m_1^2$, and

$$\tilde{h} = U^{(v)\dagger} h \quad (33)$$

is the matrix of Yukawa couplings in the mass eigenstate basis of light and heavy Majorana neutrinos. In the interesting case $M_2 - M_1 = \mathcal{O}(M_1)$ the CP asymmetry ε_1 is enhanced by a factor $\mathcal{O}(1)$. However, one then has to study the decays of both heavy neutrinos, N_1 and N_2 [19].

In the case of hierarchical neutrinos, $m_3 \simeq (\Delta m_{\text{atm}}^2)^{1/2} \gg m_2 \simeq (\Delta m_{\text{sol}}^2)^{1/2} \gg m_1$, Eq. (32) yields an upper bound on the CP asymmetry [30]

$$|\varepsilon_1| \leq \frac{3}{16\pi} \frac{M_1 (\Delta m_{\text{atm}}^2)^{1/2}}{v^2}, \quad (34)$$

where we have neglected the term $\propto \Delta m_{\text{sol}}^2$. For an inverted hierarchy $m_3 \sim m_2 \simeq (\Delta m_{\text{atm}}^2)^{1/2} \gg m_1$ and $m_3^2 - m_2^2 = \Delta m_{\text{sol}}^2$ both terms contributing to Eq. (32) are approximately equal to $(\Delta m_{\text{atm}}^2)^{1/2}$, and the upper bound is larger by a factor two. Further, for Yukawa couplings with $|h_{ij}| \leq |h_{33}| = \mathcal{O}(1)$, one has $M_3 \sim v^2/m_3$. The maximal CP asymmetry is then a measure of the hierarchy among the heavy Majorana neutrinos,

$$|\varepsilon_1|^{\text{max}} \sim 0.1 \frac{M_1}{M_3}. \quad (35)$$

It is remarkable that the upper bound (34) is frequently saturated in models with hierarchical neutrino masses (see, e.g., [22,31–36]). One reason is that in the leptonic mixing matrix $U = U^{(e)\dagger} U^{(v)}$ all elements, except U_{e3} , are known to be $\mathcal{O}(1)$. This is often explained by the structure of $U^{(v)}$, whereas $U^{(e)}$ has small off-diagonal elements. The Yukawa matrix $\tilde{h}_v = U^{(v)\dagger} h_v$ has then naturally large off-diagonal elements, even if h_v is almost diagonal. For hierarchical neutrinos the upper bound on the CP asymmetry is then easily saturated.

In terms of the quadratic mean $\bar{m}/\sqrt{3}$, with

$$\bar{m} = \sqrt{m_1^2 + m_2^2 + m_3^2}, \quad (36)$$

the bound (34) may be written as

$$|\varepsilon_1| \leq \frac{3}{16\pi} \frac{M_1 \bar{m}}{v^2}. \quad (37)$$

For quasi-degenerate neutrinos, where $m_1 \simeq m_2 \simeq m_3 \simeq \bar{m}/\sqrt{3} \gg (\Delta m_{\text{atm}}^2)^{1/2}$, one gets the stronger bound

$$|\varepsilon_1| \leq \frac{3\sqrt{3}}{16\pi} \frac{M_1 \Delta m_{\text{atm}}^2}{v^2 \bar{m}}. \quad (38)$$

There is no well defined boundary between hierarchical and quasi-degenerate neutrinos. In our analysis we shall choose $\bar{m} = 1 \text{ eV}$, such that $\bar{m}/\sqrt{3} \simeq 0.58 \text{ eV} \gg \sqrt{\Delta m_{\text{atm}}^2} \simeq 0.05 \text{ eV}$. The interesting case where all neutrinos have masses $m_i = \mathcal{O}(0.1 \text{ eV})$ will be discussed elsewhere [19].

What is the allowed range of the masses \tilde{m}_1 and M_1 which are crucial for leptogenesis? Assuming Yukawa couplings $|\tilde{h}_{ij}| \leq 1$, one has

$$M_1 \leq M_3 \sim \frac{v^2}{m_3}. \quad (39)$$

The effective neutrino mass \tilde{m}_1 is given by (cf. (29)),

$$\tilde{m}_1 = \frac{v^2}{M_1} \sum_i |\tilde{h}_{i1}^2| = \sum_i m_i |\Omega_{i1}^2|. \quad (40)$$

From the orthogonality of Ω one obtains the lower bound [37],

$$\tilde{m}_1 \geq m_1 \sum_i |\Omega_{i1}^2| \geq m_1 \sum_i \text{Re}(\Omega_{i1}^2) = m_1. \quad (41)$$

The orthogonality condition for Ω reads explicitly,

$$\text{Re}(\Omega^T \Omega)_{11} = \frac{v^2}{M_1} \sum_i \frac{1}{m_i} \text{Re}(\tilde{h}_{i1}^2) = 1. \quad (42)$$

Unless there are strong cancellations due to phase relations between different matrix elements, one then obtains

$$\tilde{m}_1 \leq m_3 \frac{v^2}{M_1} \sum_i \frac{1}{m_i} |\tilde{h}_{i1}^2| \sim m_3 \frac{v^2}{M_1} \sum_i \frac{1}{m_i} \text{Re}(\tilde{h}_{i1}^2) = m_3. \quad (43)$$

In our analysis we shall therefore emphasize the range $m_1 \leq \tilde{m}_1 \leq m_3$.

4. Constraints on neutrino parameters

In this section we shall compare the predicted baryon asymmetry with the value measured from CMB (cf. (2)), using the relation (6). Incorporating also the bound on the CP asymmetry described in the previous section will enable us to derive an allowed region for the three parameters M_1 , \tilde{m}_1 and, very interestingly, \bar{m} . Before describing the numerical results it is useful to discuss some general properties of the solutions of the kinetic equations.

The abundance $N_{N_1}(z)$ of the heavy Majorana neutrinos is independent of the asymmetry N_{B-L} . Thus, for a given solution $N_{N_1}(z)$, or equivalently $\Delta(z) = N_{N_1}(z) - N_{N_1}^{\text{eq}}(z)$, the solution for the asymmetry $N_{B-L}(z)$ reads,

$$N_{B-L}(z) = N_{B-L}(z_{\text{in}}) e^{-\int_{z_{\text{in}}}^z dz' W(z')} - \frac{3}{4} \varepsilon_1 \kappa(z; \tilde{m}_1, M_1, \bar{m}), \quad (44)$$

where $z_{\text{in}} \ll 1$, and the efficiency factor κ is given by

$$\kappa(z) = \frac{4}{3} \int_{z_{\text{in}}}^z dz' D(z') \Delta(z') e^{-\int_{z'}^z dz'' W(z'')}. \quad (45)$$

Since we assume that the initial asymmetry is zero, $N_{B-L}(z)$ is proportional to the CP asymmetry ε_1 .

A interesting, limiting case is $W = 0$ and $N_{N_1}^{\text{eq}} = 0$, i.e., $\Delta = N_{N_1}$, which corresponds to far out-of-equilibrium decays with vanishing washout. The final asymmetry then takes the form

$$N_{B-L}^0 = -\varepsilon_1 N_{N_1}(z_d), \quad (46)$$

where z_d is some temperature at which the heavy neutrinos are out of equilibrium and have not yet decayed. For an initial thermal abundance one then obtains $N_{B-L}^0 = -3\varepsilon_1/4$, and therefore $\kappa_0 = 1$. Within thermal leptogenesis this is the maximal asymmetry, and one always has $\kappa_0 \leq 1$.

In special parameter regimes it is possible to obtain explicit analytical expressions for the efficiency factor $\kappa(z; \tilde{m}_1, M_1, \bar{m})$ [22]. For small \tilde{m}_1 and \bar{m} washout effects are small. Starting from $N_1^{\text{in}} = 0$, the final asymmetry is then proportional to the generated N_1 abundance. From the reaction densities given in [25], one easily obtains at $z \ll 1$: $D \propto M_{\text{pl}} \tilde{m}_1 z^2 / v^2$ and $S \propto M_{\text{pl}} \tilde{m}_1 / v^2$. Hence, one obtains from Eq. (20),

$$\kappa \propto N_{N_1}(z_d) \propto \frac{M_{\text{pl}} \tilde{m}_1}{v^2}. \quad (47)$$

Also interesting is the case of large \tilde{m}_1 and small M_1 , where the washout is dominated by the $W - \Delta W$ term. At large temperatures, $z < 1$, the thermal N_1 abundance is then quickly reached. At small temperatures, $z > 1$, the N_1 abundance is reduced by the $\Delta L = 1$ scatterings and by the decays. The reaction densities $\gamma_{S,D}$ decrease exponentially, and the efficiency factor is determined by the N_1 abundance at freeze-out \bar{z} [22],

$$\kappa \propto N_{N_1}(\bar{z}) \propto \frac{1}{\gamma_{S,D}} \propto \frac{1}{\tilde{m}_1}. \quad (48)$$

For intermediate temperatures, i.e., $z \sim 1$, the Boltzmann equations have to be solved numerically.

4.1. Numerical results

In Fig. 5 we have plotted¹ the predicted present baryon asymmetry as a function of the parameter \tilde{m}_1 for different values of M_1 , assuming a typical value of the CP asymmetry, $\varepsilon_1 = -10^{-6}$. We have calculated the baryon asymmetry for two values of \bar{m} .

In Fig. 5(a), $\bar{m} = 0.05 \text{ eV} \simeq \sqrt{\Delta m_{\text{atm}}^2}$, which corresponds to the case of hierarchical neutrinos; $\bar{m} = 1 \text{ eV}$ in Fig. 5(b), which represents the case of quasi-degenerate neutrinos with all light neutrino masses approximately equal, $m_i = 1/\sqrt{3} \text{ eV} \simeq 0.58 \text{ eV}$. We have performed the calculations both for an initially vanishing N_1 abundance (thick lines) and for a thermal initial N_1 abundance, $N_{N_1}^{\text{in}} = 3/4$ (thin lines).

Following [22], we show in Fig. 6 the dependence of the baryon asymmetry on the

¹ All numerical results have been crosschecked by two independent codes. Figs. 1–4 and 5(b)–7(b) are based on one code; the other code has been used for Figs. 5(a)–7(a).

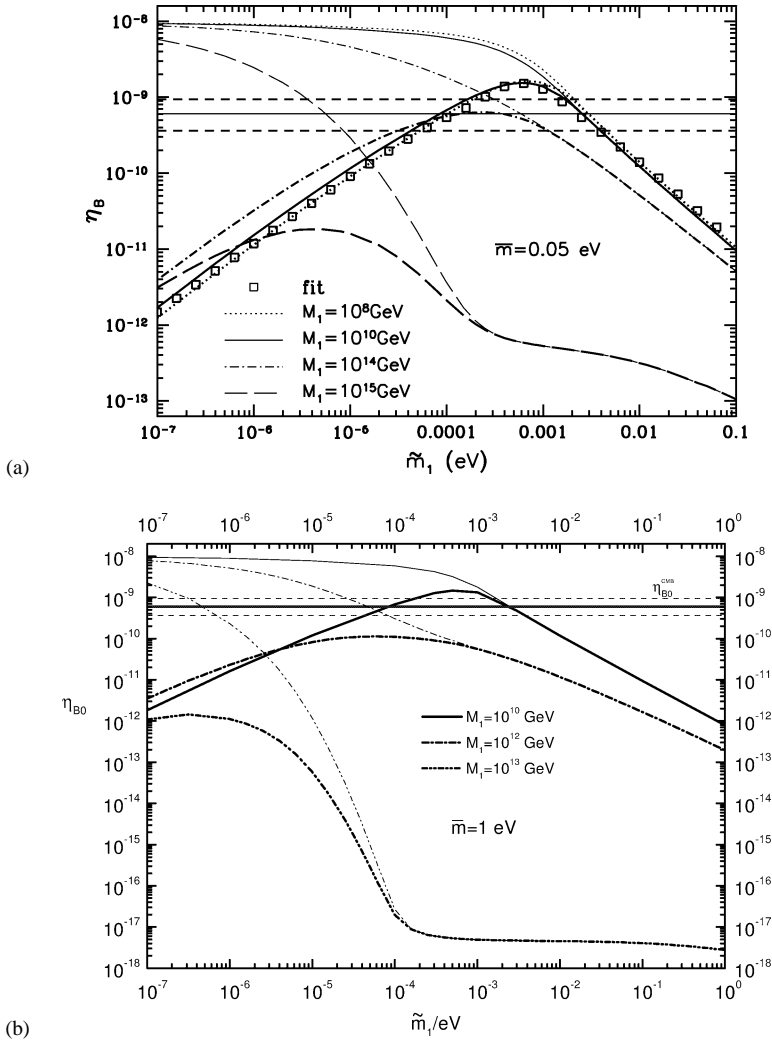


Fig. 5. Predicted baryon-to-photon ratio η_{B0} as a function of \tilde{m}_1 , for $\varepsilon_1 = -10^{-6}$ and for the indicated values of M_1 . The horizontal solid and dashed lines indicate the mean and the upper/lower values (3σ) of η_{B0}^{CMB} , respectively (see Eq. (2)). (a) Hierarchical neutrino case ($\bar{m} = 0.05$ eV $\simeq \sqrt{\Delta m_{\text{atm}}^2}$). The squares denote the fit (50). (b) Quasi-degenerate neutrino case ($m_{\nu_i} \simeq 0.58$ eV).

parameters \tilde{m}_1 and M_1 by means of iso- κ_0 curves of the efficiency parameter. Figs. 6(a) and (b) correspond to the cases $\bar{m} = 0.05$ eV and $\bar{m} = 1$ eV, respectively. For vanishing initial N_1 abundance the enclosed domains have a finite extension in \tilde{m}_1 ; for thermal initial abundance there is no boundary at small \tilde{m}_1 .

Figs. 5 and 6 clearly show the existence of two different regimes: the domain of ‘small’ N_1 masses, $M_1 < 10^{13}$ GeV $(0.1 \text{ eV}/\bar{m})^2$, and the domain of ‘large’ N_1 masses, $M_1 > 10^{13}$ GeV $(0.1 \text{ eV}/\bar{m})^2$. The dependence of the boundary on \bar{m} is determined by the

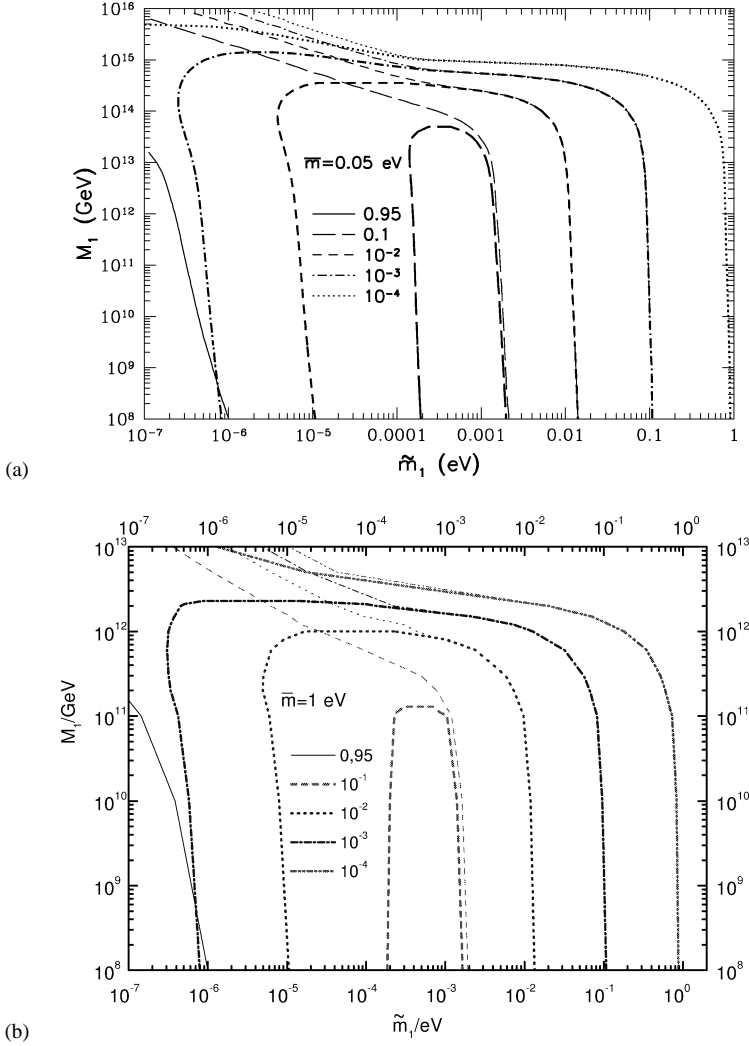


Fig. 6. Iso- κ_0 curves for $N_{N_1}^{\text{in}} = 0$ (thick lines) and $N_{N_1}^{\text{in}} = 3/4$ (thin lines). (a) Hierarchical neutrino case ($\bar{m} = 0.05$ eV $\simeq \sqrt{\Delta m_{\text{atm}}^2}$). (b) Quasi-degenerate neutrino case ($m_{v_i} \simeq 0.58$ eV).

behaviour of the non-resonant washout rate, $\Delta W \propto M_1 \bar{m}^2$. Note, that in previous studies of the washout effects [10] the obtained M_1 dependence was a result of an assumed behaviour of ΔW at $z \gg 1$. As our discussion in Section 2 shows, such an assumption is unnecessary, since the behaviour of ΔW is governed by $M_1 \bar{m}^2$.

4.1.1. Small M_1 regime

In this case the non-resonant part ΔW of the washout rate is negligible in first approximation, and there is only a small dependence on M_1 and \bar{m} in the final asymmetry.

Hence, the efficiency factor κ_0 depends approximately only on the parameter \tilde{m}_1 . From Fig. 5 one reads off that in the case of zero initial N_1 abundance the final asymmetry reaches its maximum at $\tilde{m}_1^{\text{peak}} \simeq 6 \times 10^{-4}$ eV. We can then express the baryon asymmetry in the following form,

$$\eta_{B0} = 1.5 \times 10^{-9} \frac{|\varepsilon_1|}{10^{-6}} \frac{\kappa_0(\tilde{m}_1)}{\kappa_0^{\text{peak}}}, \quad (49)$$

where $\kappa_0^{\text{peak}} \equiv \kappa_0(\tilde{m}_1^{\text{peak}}) \simeq 0.16$ is the maximal efficiency factor κ_0 obtainable for zero initial N_1 abundance.

The behaviour of the efficiency factor for small and large values of \tilde{m}_1 is known analytically (cf. (47), (48)). Approximately, one has $\kappa_0 \propto \tilde{m}_1$ for $\tilde{m}_1 \ll \tilde{m}_1^{\text{peak}}$, and $\kappa_0 \propto 1/\tilde{m}_1$ for $\tilde{m}_1 \gg \tilde{m}_1^{\text{peak}}$. A good fit for $\kappa_0(\tilde{m}_1)$ is given by the following expression,

$$\kappa_0(\tilde{m}_1) \simeq 0.24(x_- e^{-x_-} + x_+ e^{-x_+}) \quad (50)$$

with

$$x_{\pm} = \left(\frac{\tilde{m}_1}{\tilde{m}_{\pm}} \right)^{\mp 1 - \alpha}, \quad (51)$$

and $\tilde{m}_- = 3.5 \times 10^{-4}$ eV, $\tilde{m}_+ = 8.3 \times 10^{-4}$ eV, $\alpha = 0.1$. The corresponding baryon asymmetry is shown in Fig. 5(a); the fit is optimal for $M_1 = 10^8$ GeV.

In case of thermal initial N_1 abundance the maximal efficiency factor is obtained in the unphysical limit $\tilde{m}_1 \rightarrow 0$, where the heavy neutrinos decouple completely from the thermal bath. One then has

$$\eta_{B0}^{\text{max}} \simeq 0.96 \times 10^{-2} \varepsilon_1. \quad (52)$$

On the other hand, for sufficiently strong coupling of the heavy neutrinos to the thermal bath, i.e., $\tilde{m}_1 \gtrsim \tilde{m}_1^{\text{peak}}$, there is no dependence on the initial neutrino abundance, and the two cases $N_{N_1} = 0$ and $N_{N_1}^{\text{in}} = 3/4$ give the same final baryon asymmetry. In this case possible asymmetries generated in the decays of the heavier neutrinos N_2 and N_3 have also no effect on the final baryon asymmetry. Note, that in comparison with the analytical results of Ref. [22], we obtain an efficiency factor κ which is about three times smaller.

4.1.2. Large M_1 regime

In this regime the washout rate $\Delta W \propto M_1 \bar{m}^2$ dominates and the iso- κ_0 curves in the (\tilde{m}_1, M_1) -plane tend to become independent of \tilde{m}_1 with increasing M_1 . However, some dependence on \tilde{m}_1 remains due to the effect of D and S (cf. (20), (21)) on the N_1 abundance. This is why the curves never become exactly horizontal. Note, that the curves tend to converge in such a way that a small variation of M_1 leads to a large variation of the final asymmetry. In this region any small change in the kinetic equations can have large effects on the final asymmetry. On the other hand, a curve corresponding to a given value of the final asymmetry, e.g., η_{B0}^{CMB} , is rather insensitive to small changes of the kinetic equations. Thus in this region the uncertainty of ΔW at small values of z is, fortunately, not important. We therefore conclude that, within our framework of thermal leptogenesis,

we have obtained a description of the baryon asymmetry in terms of just four neutrino parameters: ε_1 , M_1 , \tilde{m}_1 and \bar{m} .

4.2. CMB constraint

The CMB constraint on neutrino parameters is given by the requirement

$$\eta_{B0} \simeq 0.96 \times 10^{-2} |\varepsilon_1| \kappa_0 (\tilde{m}_1, M_1, \bar{m}) = \eta_{B0}^{\text{CMB}}. \quad (53)$$

In the case $N_{N_1}^{\text{in}} = 0$, the substitution of the efficiency factor by its maximum κ_0^{peak} yields an important lower limit on the CP asymmetry ε_1 ,

$$|\varepsilon_1| \gtrsim 4.0 \times 10^{-7} \left(\frac{\eta_{B0}^{\text{CMB}}}{6 \times 10^{-10}} \right) \gtrsim 2.4 \times 10^{-7}. \quad (54)$$

Here the last inequality corresponds to the (3σ) lower limit for η_{B0}^{CMB} (cf. (2)). For small M_1 , the CMB bound becomes a determination of \tilde{m}_1 as function of the CP asymmetry. There are obviously two solutions: $\tilde{m}_1^- < \tilde{m}_1^{\text{peak}}$ and $\tilde{m}_1^+ > \tilde{m}_1^{\text{peak}}$. From the fit (50) one easily finds \tilde{m}_1^\mp for CP asymmetries sufficiently far above the bound (54),

$$\tilde{m}_1^- \simeq 7.9 \times 10^{-5} \text{ eV} \left(\frac{\eta_{B0}^{\text{CMB}}}{6 \times 10^{-10}} \frac{10^{-6}}{|\varepsilon_1|} \right)^{1.1}, \quad (55)$$

$$\tilde{m}_1^+ \simeq 2.8 \times 10^{-3} \text{ eV} \left(\frac{6 \times 10^{-10}}{\eta_{B0}^{\text{CMB}}} \frac{|\varepsilon_1|}{10^{-6}} \right)^{0.9}. \quad (56)$$

As ε_1 decreases to the lower bound (54), \tilde{m}_1^- and \tilde{m}_1^+ approach $\tilde{m}_1^{\text{peak}} \simeq 6 \times 10^{-4} \text{ eV}$.

In the case of a thermal initial N_1 abundance the bound (54) gets relaxed by a factor $1/k_0^{\text{peak}} \simeq 6.4$, and one obtains the usual bound for $\kappa_0 = 1$ in Eq. (53),

$$|\varepsilon_1| \gtrsim 6.3 \times 10^{-8} \left(\frac{\eta_{B0}^{\text{CMB}}}{6 \times 10^{-10}} \right) \gtrsim 3.8 \times 10^{-8}. \quad (57)$$

This bound can only be reached for $\tilde{m}_1 \ll \tilde{m}_1^{\text{peak}}$, i.e., very small values which are not easily obtained in models of neutrino masses. Note, that $\tilde{m}_1 > m_1$, the smallest neutrino mass eigenvalue [37] and that $\tilde{m}_1^{\text{peak}} \sim 0.1 \sqrt{\Delta m_{\text{sol}}^2}$. Further, one has to worry about the production mechanism of a large initial abundance of extremely weakly coupled heavy neutrinos.

4.3. CMB constraint plus CP bound

Until now we have treated the CP asymmetry ε_1 as an independent parameter. However, as discussed in Section 3, for hierarchical as well as quasi-degenerate neutrinos, the CP asymmetry satisfies an upper bound $|\varepsilon_1| < \varepsilon(M_1, \bar{m})$ (cf. Eqs. (37), (38)). Together with the CMB constraint (53) this yields the following restriction on the space of parameters \tilde{m}_1 , M_1 , and \bar{m} ,

$$\eta_{B0}^{\text{max}}(\tilde{m}_1, M_1, \bar{m}) \simeq 0.96 \times 10^{-2} \varepsilon(M_1, \bar{m}) \kappa_0(\tilde{m}_1, M_1, \bar{m}) \gtrsim \eta_{B0}^{\text{CMB}}. \quad (58)$$

For hierarchical neutrinos Eq. (37) yields the upper bound on the CP asymmetry,

$$|\varepsilon_1| < 1 \times 10^{-6} \left(\frac{M_1}{10^{10} \text{ GeV}} \right) \left(\frac{\Delta m_{\text{atm}}^2}{2.5 \times 10^{-3} \text{ eV}^2} \right)^{1/2}. \quad (59)$$

Combining this with the CMB constraint (54) yields a lower bound on M_1 [30]. For zero (thermal) initial N_1 abundance one obtains,

$$M_1 \gtrsim 2.4(0.4) \times 10^9 \text{ GeV} \left(\frac{2.5 \times 10^{-3} \text{ eV}^2}{\Delta m_{\text{atm}}^2} \right)^{1/2}. \quad (60)$$

In the case of inverted hierarchy the upper bound on the CP asymmetry is twice as large and therefore the lower bound on M_1 is twice as small.

In the case of quasi-degenerate neutrinos Eq. (38) implies a stronger bound on the CP asymmetry,

$$|\varepsilon_1| < 0.9 \times 10^{-7} \left(\frac{M_1}{10^{10} \text{ GeV}} \right) \left(\frac{1 \text{ eV}}{\bar{m}} \right) \left(\frac{\Delta m_{\text{atm}}^2}{2.5 \times 10^{-3} \text{ eV}^2} \right). \quad (61)$$

The corresponding lower bound on M_1 reads for zero (thermal) initial N_1 abundance,

$$M_1 \gtrsim 2.7(0.4) \times 10^{10} \text{ GeV} \left(\frac{\bar{m}}{1 \text{ eV}} \right) \left(\frac{2.5 \times 10^{-3} \text{ eV}^2}{\Delta m_{\text{atm}}^2} \right). \quad (62)$$

The bounds (59) and (61) on the CP asymmetry seem to suggest that by increasing M_1 any value $|\varepsilon_1| < 1$ can be reached. One may therefore expect it to be rather easy to satisfy the CMB constraint (53). However, in the regime of large M_1 the efficiency factor $\kappa_0(\tilde{m}_1, M_1, \bar{m})$ is exponentially suppressed. This dominates the linear increase of $|\varepsilon_1|^{\text{max}}$ with M_1 and leads to an upper limit on M_1 .

This situation is illustrated in Figs. 7(a) and (b), where iso- η_{B0}^{max} curves in the (\tilde{m}_1, M_1) -plane are shown for $\bar{m} = 0.05 \text{ eV}$ and $\bar{m} = 1 \text{ eV}$, respectively. In the first case we have assumed a normal hierarchy. In the second case we have used $|\varepsilon_1| < 10^{-7} M_1 / 10^{10} \text{ GeV}$ corresponding to $\Delta m_{\text{atm}}^2 \simeq 2.9 \times 10^{-3} \text{ eV}^2$. For values \tilde{m}_1 and M_1 enclosed by these curves the baryon asymmetry η_{B0}^{CMB} can be obtained. In the case of $N_{N_1}^{\text{in}} = 0$, the allowed regions are closed domains; for $N_{N_1}^{\text{in}} = 3/4$ there is no lower limit on \tilde{m}_1 .

As discussed in Section 3, the effective neutrino mass \tilde{m}_1 is bounded from below by m_1 , the mass of the lightest neutrino, and also likely to be smaller than m_3 , the mass of the heaviest neutrino. For quasi-degenerate neutrinos this implies $\tilde{m}_1 \simeq \bar{m}/\sqrt{3}$. This value is indicated by the vertical line in Fig. 7(b) from which one reaches the conclusion that quasi-degenerate neutrinos are incompatible with leptogenesis. A similar conclusion was reached in Ref. [37] based on results of [10], assuming zero initial N_1 abundance. As our analysis shows quasi-degenerate neutrinos are strongly disfavoured by thermal leptogenesis for all possible CP asymmetries and initial conditions. Possible ways to evade this conclusion are a resonant enhancement of the CP asymmetry in the case of heavy neutrino mass differences of order the decay widths, $|M_{2,3} - M_1| = \mathcal{O}(\Gamma_i)$ [38], or a completely non-thermal leptogenesis [37].

In the case of hierarchical neutrinos there is a lower bound on M_1 as function of \tilde{m}_1 , which can be read off from Fig. 7(a) in the case of a normal hierarchy, while for inverted

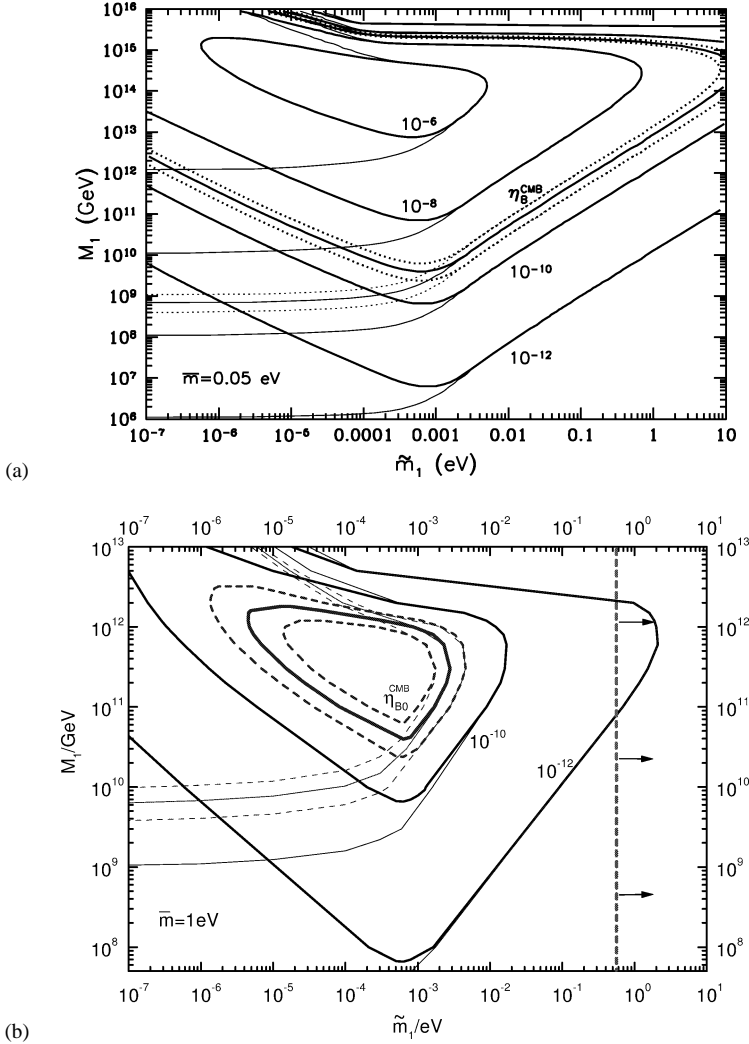


Fig. 7. Iso- η_{B0}^{\max} curves for $N_1^{\text{in}} = 0$ (thick lines) and $N_1^{\text{in}} = 3/4$ (thin lines). The region within the dashed lines is currently allowed by the CMB constraint (cf. Eq. (58)) for the (3σ) lower η_{B0}^{CMB} value. (a) Hierarchical neutrino case ($\bar{m} = 0.05$ eV $\simeq \sqrt{\Delta m_{\text{atm}}^2}$). (b) Quasi-degenerate neutrino case ($m_{\nu_i} \simeq 0.58$ eV). The dashed vertical line and the arrows refer to the bound (41).

hierarchy this bound is twice as small. No upper bound stronger than $M_3 \sim 10^{15}$ GeV exists. For thermal initial conditions all values of $\tilde{m}_1 < m_3$ are allowed.

Comparing Figs. 7(a) and (b), it is evident that a more stringent upper limit than 1 eV exists for \bar{m} . The determination of this precise bound goes beyond the goal of this paper and is left for future work [19].

Any point in the space $(\eta_{B0}, \tilde{m}_1, M_1)$ which lies below the surface η_{B0}^{\max} and above the plane η_{B0}^{CMB} represents a possible set of neutrino parameters with some value $|\varepsilon_1| \leq |\varepsilon_1|^{\max}$. As discussed in Section 3, in many models one has $|\varepsilon_1| \sim |\varepsilon_1|^{\max}$. The CMB bound then yields a precise relation between \tilde{m}_1 and M_1 . In particular, for the interesting range $0.1 \text{ eV} \gtrsim \tilde{m}_1 \gtrsim \tilde{m}_1^{\text{peak}} \simeq 6 \times 10^{-4} \text{ eV}$, one has the simple relation,

$$M_1 \simeq 3 \times 10^{10} \text{ GeV} \left(\frac{\tilde{m}_1}{0.01 \text{ eV}} \right). \quad (63)$$

This corresponds to the scenario originally proposed in [31], with $\tilde{m}_1 \sim \sqrt{\Delta m_{\text{sol}}^2} \sim 0.005 \text{ eV}$, where we have assumed the LMA solution [39]. The corresponding baryogenesis temperature is $T_B \sim M_1 \sim 10^{10} \text{ GeV}$.

5. Conclusions

We have studied in some detail the minimal version of thermal leptogenesis. In this framework the decays of N_1 , the lightest of the heavy Majorana neutrinos, are the source of the baryon asymmetry, and only Yukawa interactions generate the initial heavy neutrino abundance; further, the connection between light and heavy neutrinos is given by the seesaw mechanism. The final baryon asymmetry is then determined by only four parameters: the CP asymmetry ε_1 , the heavy neutrino mass M_1 , the effective light neutrino mass \tilde{m}_1 and the quadratic mean \bar{m} of the light neutrino masses.

The constraint from the cosmic microwave background on the baryon asymmetry strongly restricts the allowed range of neutrino parameters. For small values of M_1 , the efficiency factor κ depends only on \tilde{m}_1 . Together with the upper bound on the CP asymmetry, this yields an important lower bound on M_1 and therefore on the baryogenesis temperature, $T_B \sim M_1 \gtrsim 2.4 \times 10^9 \text{ GeV}$.

For large values of M_1 , washout effects, proportional to $M_1 \bar{m}^2$, become important. This leads to the conclusion that the case of quasi-degenerate neutrinos, $\bar{m} \gg \sqrt{\Delta m_{\text{atm}}^2}$, is incompatible with thermal leptogenesis. On the other hand, in the case of hierarchical neutrinos, the full range of light and heavy neutrino masses considered in grand unified theories is viable. The intermediate regime, $m_i = \mathcal{O}(0.1 \text{ eV})$, remains to be studied in detail.

Global fits of solar and atmospheric neutrino data indicate large mixing angles for neutrino oscillations in both cases. With respect to neutrino masses, leptogenesis favours the possible case of a mild hierarchy, $m_2 \simeq \sqrt{\Delta m_{\text{sol}}^2} \simeq 0.1 \sqrt{\Delta m_{\text{atm}}^2} \simeq 0.1 m_3$. Due to the large mixing angles, a priori possibility $m_1 \ll m_2$ appears unlikely. With $m_1 \leq \tilde{m}_1 \lesssim m_3$, one then arrives at the conclusion $\tilde{m}_1 \sim 0.1 \sqrt{\Delta m_{\text{atm}}^2}$. Furthermore, in many of the recently discussed models for neutrino masses the CP asymmetry ε_1 is close to its upper bound. This finally determines the heavy neutrino mass M_1 and the baryogenesis temperature to be $T_B \sim M_1 = \mathcal{O}(10^{10} \text{ GeV})$.

The unfortunate prediction of thermal leptogenesis is that the search for absolute neutrino masses in tritium β -decay and CMB combined with Large Scale Structure will

be unsuccessful in the near future. Our present bound, $\sum_i m_i < \sqrt{3} \text{ eV}$, can still be significantly improved [19]. However, the search for neutrinoless double β -decay with a sensitivity $|m_{ee}| = \mathcal{O}(\sqrt{\Delta m_{\text{atm}}^2})$ [40] may very well be successful.

Acknowledgements

P.D.B. was supported by the Alexander von Humboldt foundation; M.P. was supported by the EU network “Supersymmetry and the Early Universe” under contract No. HPRN-CT-2000-00152. We wish to thank S. Davidson, S. Huber, A. Ibarra, H.B. Nielsen, Q. Shafi and Y. Takahashi for useful discussions.

References

- [1] V.A. Rubakov, M.E. Shaposhnikov, Phys. Usp. 39 (1996) 461.
- [2] M. Quiros, Nucl. Phys. Proc. Suppl. 101 (2001) 401.
- [3] T. Yanagida, in: Workshop on Unified Theories, KEK report 79-18, 1979, p. 95;
M. Gell-Mann, P. Ramond, Y. Slansky, in: P. van Nieuwenhuizen, D. Freedman (Eds.), Supergravity, North-Holland, Amsterdam, 1979, p. 315.
- [4] V.A. Kuzmin, V.A. Rubakov, M.E. Shaposhnikov, Phys. Lett. B 155 (1985) 36.
- [5] D. Bödeker, G.D. Moore, K. Rummukainen, Phys. Rev. D 61 (2000) 056003.
- [6] E.W. Kolb, M.S. Turner, The Early Universe, Addison–Wesley, New York, 1990.
- [7] M. Fukugita, T. Yanagida, Phys. Lett. B 174 (1986) 45.
- [8] M.A. Luty, Phys. Rev. D 45 (1992) 455.
- [9] M. Plümacher, Z. Phys. C 74 (1997) 549.
- [10] For a review and references, see: W. Buchmüller, M. Plümacher, Int. J. Mod. Phys. A 15 (2000) 5047.
- [11] P. de Bernardis, et al., Astrophys. J. 564 (2002) 559.
- [12] C. Pryke, et al., Astrophys. J. 568 (2002) 46.
- [13] R. Stompor, et al., Astrophys. J. 561 (2001) L7.
- [14] J.L. Sievers, et al., astro-ph/0205387.
- [15] http://map.gsfc.nasa.gov/m_mm/ms_status.html.
- [16] G. Jungman, M. Kamionkowski, A. Kosowsky, D.N. Spergel, Phys. Rev. D 54 (1996) 1332;
M. Zaldarriaga, D.N. Spergel, U. Seljak, Astrophys. J. 488 (1997) 1.
- [17] <http://astro.estec.esa.nl/Planck/>.
- [18] B.D. Fields, S. Sarkar, in: Review of Particle Physics, Phys. Rev. D 66 (2002) 010001.
- [19] W. Buchmüller, P. Di Bari, M. Plümacher, in preparation.
- [20] H.B. Nielsen, Y. Takahashi, Phys. Lett. B 507 (2001) 241, hep-ph/0205180.
- [21] W. Buchmüller, S. Fredenhagen, Phys. Lett. B 483 (2000) 217.
- [22] R. Barbieri, P. Creminelli, A. Strumia, N. Tetradis, Nucl. Phys. B 575 (2000) 61.
- [23] W. Buchmüller, M. Plümacher, Phys. Lett. B 511 (2001) 74.
- [24] S.Yu. Khlebnikov, M.E. Shaposhnikov, Nucl. Phys. B 308 (1988) 885;
J.A. Harvey, M.S. Turner, Phys. Rev. D 42 (1990) 3344.
- [25] M. Plümacher, Nucl. Phys. B 530 (1998) 207.
- [26] J.A. Casas, A. Ibarra, Nucl. Phys. B 618 (2001) 171.
- [27] M. Flanz, E.A. Paschos, U. Sarkar, Phys. Lett. B 345 (1995) 248;
M. Flanz, E.A. Paschos, U. Sarkar, Phys. Lett. B 384 (1996) 487, Erratum.
- [28] L. Covi, E. Roulet, F. Vissani, Phys. Lett. B 384 (1996) 169.
- [29] W. Buchmüller, M. Plümacher, Phys. Lett. B 431 (1998) 354.
- [30] S. Davidson, A. Ibarra, hep-ph/0202239.

- [31] W. Buchmüller, M. Plümacher, Phys. Lett. B 389 (1996) 73.
- [32] S. Lola, G.G. Ross, Nucl. Phys. B 553 (1999) 81.
- [33] W. Buchmüller, T. Yanagida, Phys. Lett. B 445 (1999) 399.
- [34] W. Buchmüller, D. Wyler, Phys. Lett. B 521 (2001) 291.
- [35] M.S. Berger, K. Siyeon, Phys. Rev. D 65 (2002) 053019.
- [36] D. Falcone, Phys. Rev. D 65 (2002) 077301.
- [37] M. Fujii, K. Hamaguchi, T. Yanagida, hep-ph/0202210.
- [38] A. Pilaftsis, Int. J. Mod. Phys. A 14 (1999) 1811.
- [39] J.N. Bahcall, M.C. Gonzalez-Garcia, C. Peña-Garay, JHEP 0108 (2001) 014.
- [40] H.V. Klapdor-Kleingrothaus, Nucl. Phys. Suppl. 100 (2001) 350.